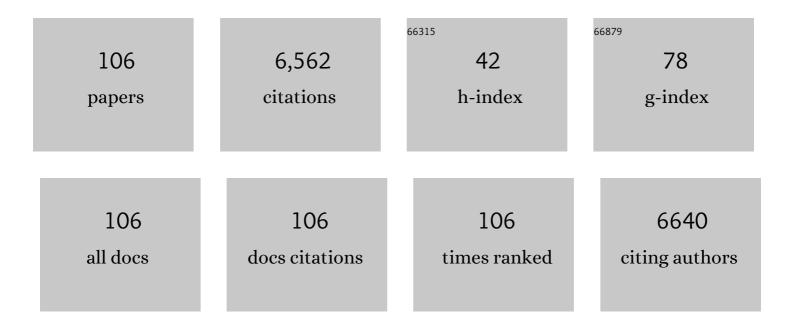
List of Publications by Year in descending order

Source: https://exaly.com/author-pdf/6419759/publications.pdf Version: 2024-02-01



#	Article	IF	CITATIONS
1	Synergistic coupling of CoFe-LDH arrays with NiFe-LDH nanosheet for highly efficient overall water splitting in alkaline media. Applied Catalysis B: Environmental, 2019, 253, 131-139.	10.8	503
2	Perovskite oxide ultrathin nanosheets/g-C3N4 2D-2D heterojunction photocatalysts with significantly enhanced photocatalytic activity towards the photodegradation of tetracycline. Applied Catalysis B: Environmental, 2017, 201, 617-628.	10.8	360
3	Novel p–n heterojunction photocatalyst constructed by porous graphite-like C3N4 and nanostructured BiOI: facile synthesis and enhanced photocatalytic activity. Dalton Transactions, 2013, 42, 15726.	1.6	333
4	Two-Dimensional Caln <sub>2</sub> S <sub>4</sub> /g-C <sub>3</sub> N <sub>4</sub> Heterojunction Nanocomposite with Enhanced Visible-Light Photocatalytic Activities: Interfacial Engineering and Mechanism Insight. ACS Applied Materials & Interfaces, 2015, 7, 19234-19242.	4.0	307
5	Modifiers-assisted formation of nickel nanoparticles and their catalytic application to p-nitrophenol reduction. CrystEngComm, 2013, 15, 560-569.	1.3	244
6	Construction of SnNb 2 O 6 nanosheet/g-C 3 N 4 nanosheet two-dimensional heterostructures with improved photocatalytic activity: Synergistic effect and mechanism insight. Applied Catalysis B: Environmental, 2016, 183, 113-123.	10.8	239
7	Synthesis of redox-mediator-free direct Z-scheme AgI/WO3 nanocomposite photocatalysts for the degradation of tetracycline with enhanced photocatalytic activity. Chemical Engineering Journal, 2016, 300, 280-290.	6.6	229
8	Ag <sub>2</sub> S/g-C <sub>3</sub> N <sub>4</sub> composite photocatalysts for efficient Pt-free hydrogen production. The co-catalyst function of Ag/Ag <sub>2</sub> S formed by simultaneous photodeposition. Dalton Transactions, 2014, 43, 4878-4885.	1.6	203
9	Enhancement of g-C 3 N 4 nanosheets photocatalysis by synergistic interaction of ZnS microsphere and RGO inducing multistep charge transfer. Applied Catalysis B: Environmental, 2016, 198, 200-210.	10.8	165
10	A new visible light active multifunctional ternary composite based on TiO2–In2O3 nanocrystals heterojunction decorated porous graphitic carbon nitride for photocatalytic treatment of hazardous pollutant and H2 evolution. Applied Catalysis B: Environmental, 2015, 170-171, 195-205.	10.8	160
11	Hydrothermal synthesis of In 2 S 3 /g-C 3 N 4 heterojunctions with enhanced photocatalytic activity. Journal of Colloid and Interface Science, 2014, 433, 9-15.	5.0	159
12	Highly efficient heterojunction photocatalyst based on nanoporous g-C3N4 sheets modified by Ag3PO4 nanoparticles: Synthesis and enhanced photocatalytic activity. Journal of Colloid and Interface Science, 2014, 417, 115-120.	5.0	143
13	Bimetallic Co-Mo nitride nanosheet arrays as high-performance bifunctional electrocatalysts for overall water splitting. Chemical Engineering Journal, 2021, 411, 128433.	6.6	143
14	A g-C <sub>3</sub> N <sub>4</sub> /nanocarbon/Znln <sub>2</sub> S <sub>4</sub> nanocomposite: an artificial Z-scheme visible-light photocatalytic system using nanocarbon as the electron mediator. Chemical Communications, 2015, 51, 17144-17147.	2.2	136
15	RGO-Promoted All-Solid-State g-C <sub>3</sub> N <sub>4</sub> /BiVO <sub>4</sub> Z-Scheme Heterostructure with Enhanced Photocatalytic Activity toward the Degradation of Antibiotics. Industrial & Engineering Chemistry Research, 2017, 56, 8823-8832.	1.8	116
16	Enhanced photocatalytic activity of graphitic carbon nitride/carbon nanotube/Bi2WO6 ternary Z-scheme heterojunction with carbon nanotube as efficient electron mediator. Journal of Colloid and Interface Science, 2018, 512, 693-700.	5.0	101
17	In-situ ion exchange synthesis of hierarchical Agl/BiOI microsphere photocatalyst with enhanced photocatalytic properties. CrystEngComm, 2013, 15, 7556.	1.3	100
18	CoP <sub>3</sub> /CoMoP Heterogeneous Nanosheet Arrays as Robust Electrocatalyst for pH-Universal Hydrogen Evolution Reaction. ACS Sustainable Chemistry and Engineering, 2019, 7, 9309-9317.	3.2	97

#	Article	IF	CITATIONS
19	Construction of cobalt sulfide/graphitic carbon nitride hybrid nanosheet composites for high performance supercapacitor electrodes. Journal of Alloys and Compounds, 2017, 706, 41-47.	2.8	91
20	Construction of RGO/CdIn 2 S 4 /g-C 3 N 4 ternary hybrid with enhanced photocatalytic activity for the degradation of tetracycline hydrochloride. Applied Surface Science, 2018, 433, 388-397.	3.1	91
21	2020 Roadmap on two-dimensional nanomaterials for environmental catalysis. Chinese Chemical Letters, 2019, 30, 2065-2088.	4.8	90
22	N-doped graphene quantum dots as an effective photocatalyst for the photochemical synthesis of silver deposited porous graphitic C <sub>3</sub> N <sub>4</sub> nanocomposites for nonenzymatic electrochemical H <sub>2</sub> O <sub>2</sub> sensing. RSC Advances, 2014, 4, 16163-16171.	1.7	72
23	2D/2D heterojunctions of WO <sub>3</sub> nanosheet/K <sup>+</sup> Ca <sub>2</sub> Nb <sub>3</sub> O <sub>10</sub> <sup>â^²</sup> ultrathin nanosheet with improved charge separation efficiency for significantly boosting photocatalysis. Catalysis Science and Technology, 2017, 7, 3481-3491.	2.1	68
24	Integrating Ru-modulated CoP nanosheets binary co-catalyst with 2D g-C3N4 nanosheets for enhanced photocatalytic hydrogen evolution activity. Journal of Colloid and Interface Science, 2021, 585, 108-117.	5.0	67
25	Synergistic Integration of AuCu Co-Catalyst with Oxygen Vacancies on TiO <sub>2</sub> for Efficient Photocatalytic Conversion of CO <sub>2</sub> to CH <sub>4</sub> . ACS Applied Materials & Interfaces, 2021, 13, 46772-46782.	4.0	65
26	Engineering Ni(OH) <sub>2</sub> Nanosheet on CoMoO <sub>4</sub> Nanoplate Array as Efficient Electrocatalyst for Oxygen Evolution Reaction. ACS Sustainable Chemistry and Engineering, 2018, 6, 16086-16095.	3.2	64
27	Photocatalytic reduction of CO2 into CH4 over Ru-doped TiO2: Synergy of Ru and oxygen vacancies. Journal of Colloid and Interface Science, 2022, 608, 2809-2819.	5.0	63
28	Hydrogen peroxide sensing using Cu2O nanocubes decorated by Ag-Au alloy nanoparticles. Journal of Alloys and Compounds, 2017, 690, 1-7.	2.8	60
29	MoS2/SnNb2O6 2D/2D nanosheet heterojunctions with enhanced interfacial charge separation for boosting photocatalytic hydrogen evolution. Journal of Colloid and Interface Science, 2019, 536, 1-8.	5.0	60
30	Construction of novel WO3/SnNb2O6 hybrid nanosheet heterojunctions as efficient Z-scheme photocatalysts for pollutant degradation. Journal of Colloid and Interface Science, 2017, 506, 93-101.	5.0	57
31	Fe-doped NiCoP/Prussian blue analog hollow nanocubes as an efficient electrocatalyst for oxygen evolution reaction. Electrochimica Acta, 2021, 367, 137492.	2.6	56
32	SrTiO <sub>3</sub> Nanoparticle/SnNb <sub>2</sub> O <sub>6</sub> Nanosheet 0D/2D Heterojunctions with Enhanced Interfacial Charge Separation and Photocatalytic Hydrogen Evolution Activity. ACS Sustainable Chemistry and Engineering, 2017, 5, 9749-9757.	3.2	54
33	Interfacial Engineering of the Co <sub><i>x</i></sub> P–Fe <sub>2</sub> P Heterostructure for Efficient and Robust Electrochemical Overall Water Splitting. ACS Sustainable Chemistry and Engineering, 2021, 9, 7737-7748.	3.2	54
34	CdIn <sub>2</sub> S <sub>4</sub> /g-C <sub>3</sub> N <sub>4</sub> heterojunction photocatalysts: enhanced photocatalytic performance and charge transfer mechanism. RSC Advances, 2017, 7, 231-237.	1.7	52
35	Construction of CuO quantum Dots/WO3 nanosheets 0D/2D Z-scheme heterojunction with enhanced photocatalytic CO2 reduction activity under visible-light. Journal of Alloys and Compounds, 2021, 858, 157668.	2.8	51
36	Synergistically coupling of Fe-doped CoP nanocubes with CoP nanosheet arrays towards enhanced and robust oxygen evolution electrocatalysis. Journal of Colloid and Interface Science, 2021, 591, 67-75.	5.0	49

#	Article	IF	CITATIONS
37	Oxygen vacancy engineering of BiOBr/HNb3O8 Z-scheme hybrid photocatalyst for boosting photocatalytic conversion of CO2. Journal of Colloid and Interface Science, 2021, 599, 245-254.	5.0	49
38	Graphene‣ensitized Perovskite Oxide Monolayer Nanosheets for Efficient Photocatalytic Reaction. Advanced Functional Materials, 2018, 28, 1806284.	7.8	48
39	Shape-controlled synthesis of F-substituted hydroxyapatite microcrystals in the presence of Na2EDTA and citric acid. Journal of Colloid and Interface Science, 2010, 350, 30-38.	5.0	47
40	Coupling Co2P and CoP nanoparticles with copper ions incorporated Co9S8 nanowire arrays for synergistically boosting hydrogen evolution reaction electrocatalysis. Journal of Colloid and Interface Science, 2019, 550, 10-16.	5.0	47
41	ZnS microsphere/g-C <sub>3</sub> N <sub>4</sub> nanocomposite photo-catalyst with greatly enhanced visible light performance for hydrogen evolution: synthesis and synergistic mechanism study. RSC Advances, 2014, 4, 62223-62229.	1.7	46
42	Nickel–manganese bimetallic phosphides porous nanosheet arrays as highly active bifunctional hydrogen and oxygen evolution electrocatalysts for overall water splitting. Electrochimica Acta, 2020, 329, 135121.	2.6	43
43	Synthesis of novel metal nanoparitcles/SnNb2O6 nanosheets plasmonic nanocomposite photocatalysts with enhanced visible-light photocatalytic activity and mechanism insight. Journal of Alloys and Compounds, 2016, 685, 647-655.	2.8	41
44	MOF-derived cobalt oxides nanoparticles anchored on CoMoO4 as a highly active electrocatalyst for oxygen evolution reaction. Journal of Alloys and Compounds, 2019, 806, 1097-1104.	2.8	41
45	Hierarchically structured Co3O4@glucose-modified LDH architectures for high-performance supercapacitors. Applied Surface Science, 2019, 488, 639-647.	3.1	40
46	Carbon nanodots as reductant and stabilizer for one-pot sonochemical synthesis of amorphous carbon-supported silver nanoparticles for electrochemical nonenzymatic H2O2 sensing. Journal of Electroanalytical Chemistry, 2014, 728, 26-33.	1.9	39
47	Construction of ultrafine TiO <sub>2</sub> nanoparticle and SnNb <sub>2</sub> O <sub>6</sub> nanosheet 0D/2D heterojunctions with abundant interfaces and significantly improved photocatalytic activity. Catalysis Science and Technology, 2017, 7, 2308-2317.	2.1	39
48	2D/2D BiOCl/K+Ca2Nb3O10â <sup>~</sup> heterostructure with Z-scheme charge carrier transfer pathways for tetracycline degradation under simulated solar light. Applied Surface Science, 2019, 466, 863-873.	3.1	39
49	Synergistically integrated Co9S8@NiFe-layered double hydroxide core-branch hierarchical architectures as efficient bifunctional electrocatalyst for water splitting. Journal of Colloid and Interface Science, 2021, 604, 680-690.	5.0	39
50	Iron-doped nickle cobalt ternary phosphide hyperbranched hierarchical arrays for efficient overall water splitting. Electrochimica Acta, 2020, 334, 135633.	2.6	38
51	Ag nanoparticle-decorated CoS nanosheet nanocomposites: a high-performance material for multifunctional applications in photocatalysis and supercapacitors. RSC Advances, 2016, 6, 55039-55045.	1.7	36
52	Covalently Bonded Bi <sub>2</sub> O <sub>3</sub> Nanosheet/Bi <sub>2</sub> WO <sub>6</sub> Network Heterostructures for Efficient Photocatalytic CO <sub>2</sub> Reduction. ACS Applied Energy Materials, 2020, 3, 12194-12203.	2.5	34
53	Hierarchical NiCo2O4@Ni(OH)2 core-shell nanoarrays as advanced electrodes for asymmetric supercapacitors with high energy density. Journal of Alloys and Compounds, 2019, 771, 784-792.	2.8	33
54	Facile synthesis of hierarchical NiCoP nanosheets/NiCoP nanocubes homojunction electrocatalyst for highly efficient and stable hydrogen evolution reaction. Applied Surface Science, 2021, 565, 150537.	3.1	33

#	Article	IF	CITATIONS
55	The synthesis of a novel Ag–NaTaO3 hybrid with plasmonic photocatalytic activity under visible-light. CrystEngComm, 2014, 16, 1384.	1.3	31
56	Novel Zn0.8Cd0.2S/g-C3N4 heterojunctions with superior visible-light photocatalytic activity: Hydrothermal synthesis and mechanism study. Journal of Molecular Catalysis A, 2014, 395, 261-268.	4.8	30
57	Enhanced non-enzymatic electrochemical sensing of hydrogen peroxide based on Cu 2 O nanocubes/Ag-Au alloy nanoparticles by incorporation of RGO nanosheets. Journal of Electroanalytical Chemistry, 2017, 791, 23-28.	1.9	29
58	Fe-Doped CoP holey nanosheets as bifunctional electrocatalysts for efficient hydrogen and oxygen evolution reactions. International Journal of Hydrogen Energy, 2021, 46, 26391-26401.	3.8	28
59	Synergistically Integrating Nickel Porous Nanosheets with 5d Transition Metal Oxides Enabling Efficient Electrocatalytic Overall Water Splitting. Inorganic Chemistry, 2021, 60, 8189-8199.	1.9	27
60	KCa2Nb3O10/ZnIn2S4 nanosheet heterojunctions with improved charge separation efficiency for efficient photocatalytic CO2 reduction. Journal of Alloys and Compounds, 2021, 865, 158836.	2.8	27
61	Ru-doping modulated cobalt phosphide nanoarrays as efficient electrocatalyst for hydrogen evolution rection. Journal of Colloid and Interface Science, 2022, 625, 457-465.	5.0	27
62	Synthesis of cuprous oxide with morphological evolution from truncated octahedral to spherical structures and their size and shape-dependent photocatalytic activities. Journal of Colloid and Interface Science, 2016, 461, 25-31.	5.0	26
63	Construction of novel Sr0.4H1.2Nb2O6·H2O/g-C3N4 heterojunction with enhanced visible light photocatalytic activity for hydrogen evolution. Journal of Colloid and Interface Science, 2018, 526, 451-458.	5.0	26
64	Dion–Jacobson-type perovskite KCa <sub>2</sub> Ta <sub>3</sub> O <sub>10</sub> nanosheets hybridized with g-C <sub>3</sub> N <sub>4</sub> nanosheets for photocatalytic H <sub>2</sub> production. Catalysis Science and Technology, 2018, 8, 3767-3773.	2.1	26
65	Integration of ZnCo2S4 nanowires arrays with NiFe-LDH nanosheet as water dissociation promoter for enhanced electrocatalytic hydrogen evolution. Electrochimica Acta, 2019, 324, 134861.	2.6	26
66	Synergistic effects of surface Lewis Base/Acid and nitrogen defect in MgAl layered double Oxides/Carbon nitride heterojunction for efficient photoreduction of carbon dioxide. Applied Surface Science, 2021, 563, 150369.	3.1	26
67	Synergistically Coupled CoMo/CoMoP Electrocatalyst for Highly Efficient and Stable Overall Water Splitting. Inorganic Chemistry, 2022, 61, 8328-8338.	1.9	26
68	Novel Au/CaIn2S4 nanocomposites with plasmon-enhanced photocatalytic performance under visible light irradiation. Applied Surface Science, 2017, 396, 430-437.	3.1	25
69	Facile synthesis of core–shell–satellite Ag/C/Ag nanocomposites using carbon nanodots as reductant and their SERS properties. CrystEngComm, 2013, 15, 6305.	1.3	24
70	Interfacial engineering of Co3FeN embedded N-doped carbon nanoarray derived from metal–organic frameworks for enhanced oxygen evolution reaction. Electrochimica Acta, 2020, 354, 136629.	2.6	24
71	Heterostructure arrays of (Ni,Co)Se2 nanowires integrated with MOFs-derived CoSe2 dodecahedra for synergistically high-efficiency and stable overall water splitting. Applied Surface Science, 2022, 592, 153352.	3.1	24
72	Accelerating water dissociation kinetic in Co9S8 electrocatalyst by mn/N Co-doping toward efficient alkaline hydrogen evolution. International Journal of Hydrogen Energy, 2021, 46, 7989-8001.	3.8	23

#	Article	IF	CITATIONS
73	Steering Multistep Charge Transfer for Highly Selectively Photocatalytic Reduction of CO <sub>2</sub> into CH <sub>4</sub> over Pd/Cu <sub>2</sub> O/TiO <sub>2</sub> Ternary Hybrid. Solar Rrl, 2021, 5, 2000813.	3.1	23
74	Synthesis of an iron-doped 3D-ordered mesoporous cobalt phosphide material toward efficient electrocatalytic overall water splitting. Inorganic Chemistry Frontiers, 2020, 7, 3002-3010.	3.0	22
75	Oxygen-doped hollow, porous NiCoP nanocages derived from Ni–Co prussian blue analogs for oxygen evolution. Chemical Communications, 2021, 57, 8158-8161.	2.2	22
76	Interfacial engineering of CeO <sub>2</sub> on NiCoP nanoarrays for efficient electrocatalytic oxygen evolution. Nanotechnology, 2021, 32, 195704.	1.3	22
77	Interfacing Co3Mo with CoMoOx for synergistically boosting electrocatalytic hydrogen and oxygen evolution reactions. Chemical Engineering Journal, 2022, 431, 133240.	6.6	22
78	Synthesis and size-dependent electrochemical nonenzymatic H2O2 sensing of cuprous oxide nanocubes. RSC Advances, 2015, 5, 82496-82502.	1.7	21
79	Holey Cobalt–Iron Nitride Nanosheet Arrays as High-Performance Bifunctional Electrocatalysts for Overall Water Splitting. ACS Applied Materials & Interfaces, 2020, 12, 29253-29263.	4.0	21
80	Synergy of nitrogen vacancies and Fe2P cocatalyst on graphitic carbon nitride for boosting photocatalytic CO2 conversion. Chemical Engineering Journal, 2022, 446, 137096.	6.6	19
81	Regulating photocatalytic CO2 reduction selectivity via steering cascade multi-step charge transfer pathways in 1ÂT/2H-WS2/TiO2 heterojuncitons. Chemical Engineering Journal, 2022, 447, 137485.	6.6	19
82	Plasmonic Au Nanoparticles/KCa2Nb3O10 nanosheets 0D/2D heterojunctions with enhanced photocatalytic activity towards the degradation of tetracycline hydrochloride. Journal of Alloys and Compounds, 2018, 762, 38-45.	2.8	17
83	Hierarchical CoO@Ni(OH) <sub>2</sub> core–shell heterostructure arrays for advanced asymmetric supercapacitors. Nanotechnology, 2020, 31, 405705.	1.3	17
84	Iron and nitrogen Co-doped CoSe <sub>2</sub> nanosheet arrays for robust electrocatalytic water oxidation. Inorganic Chemistry Frontiers, 2021, 8, 2725-2734.	3.0	16
85	Carbon vacancy-mediated exciton dissociation in Ti3C2Tx/g-C3N4 Schottky junctions for efficient photoreduction of CO2. Journal of Colloid and Interface Science, 2022, 623, 487-499.	5.0	16
86	Novel β-In <sub>2.77</sub> S <sub>4</sub> nanosheet-assembled hierarchical microspheres: synthesis and high performance for photocatalytic reduction of Cr( <scp>vi</scp> ). RSC Advances, 2016, 6, 18227-18234.	1.7	14
87	Hierarchical urchin-like Co <sub>9</sub> S <sub>8</sub> @Ni(OH) <sub>2</sub> heterostructures with superior electrochemical performance for hybrid supercapacitors. New Journal of Chemistry, 2019, 43, 8444-8451.	1.4	14
88	Template confined construction of Fe–NiCoP/NiCoP/NF heterostructures for highly efficient electrocatalytic oxygen evolution reaction. International Journal of Hydrogen Energy, 2021, 46, 37746-37756.	3.8	14
89	0D ultrafine ruthenium quantum dot decorated 3D porous graphitic carbon nitride with efficient charge separation and appropriate hydrogen adsorption capacity for superior photocatalytic hydrogen evolution. Dalton Transactions, 2021, 50, 2414-2425.	1.6	13
90	Synergistically enhancing electrocatalytic activity of Co2P by Cr doping and P vacancies for overall water splitting. Applied Surface Science, 2022, 600, 154099.	3.1	13

#	Article	IF	CITATIONS
91	Facile synthesis and characterisation of hexagonal magnetite nanoplates. Micro and Nano Letters, 2013, 8, 383-385.	0.6	12
92	Holey defected TiO2 nanosheets with oxygen vacancies for efficient photocatalytic hydrogen production from water splitting. Surfaces and Interfaces, 2021, 23, 100979.	1.5	12
93	Anchoring RuSe2 on CoSe2 nanoarrays as a hybrid catalyst for efficient and robust oxygen evolution reaction. Journal of Colloid and Interface Science, 2022, 615, 327-334.	5.0	12
94	Photoenhanced degradation of rhodamine blue on monometallic gold (Au) loaded brookite titania photocatalysts activated by visible light. Reaction Kinetics, Mechanisms and Catalysis, 2012, 107, 487-502.	0.8	11
95	Designing positive electrodes based on 3D hierarchical CoMn <sub>2</sub> O <sub>4</sub> @NiMn-LDH nanoarray composites for high energy and power density supercapacitors. CrystEngComm, 2020, 22, 6864-6875.	1.3	11
96	Highly dispersed ultra-fine Ru nanoparticles anchored on nitrogen-doped carbon sheets for efficient hydrogen evolution reaction with a low overpotential. Journal of Alloys and Compounds, 2021, 864, 158174.	2.8	11
97	Metal–Organic Framework-Derived Three-Dimensional Macropore Nitrogen-Doped Carbon Frameworks Decorated with Ultrafine Ru-Based Nanoparticles for Overall Water Splitting. Inorganic Chemistry, 2022, 61, 9685-9692.	1.9	10
98	Iron and chromium co-doped cobalt phosphide porous nanosheets as robust bifunctional electrocatalyst for efficient water splitting. Nanotechnology, 2022, 33, 075204.	1.3	9
99	Stable and enhanced electrochemical performance based on hierarchical core–shell structure of CoMn <sub>2</sub> O <sub>4</sub> @Ni <sub>3</sub> S <sub>2</sub> electrode for hybrid supercapacitor. Nanotechnology, 2022, 33, 095707.	1.3	9
100	Synthesis and electrochemical performance of LiFePO4/C cathode materials from Fe2O3 for high-power lithium-ion batteries. Ionics, 2017, 23, 377-384.	1.2	8
101	Noble-metal-free Mo2C co-catalsyt modified perovskite oxide nanosheet photocatalysts with enhanced hydrogen evolution performance. Colloids and Surfaces A: Physicochemical and Engineering Aspects, 2021, 615, 126252.	2.3	8
102	CdS nanoparticles decorated K+Ca2Nb3O10â^' nanosheets with enhanced photocatalytic activity. Materials Letters, 2018, 229, 236-239.	1.3	7
103	Co(OH) <sub>2</sub> water oxidation cocatalyst-decorated CdS nanowires for enhanced photocatalytic CO <sub>2</sub> reduction performance. Dalton Transactions, 2021, 50, 10159-10167.	1.6	4
104	Synthesis, Crystal Structure, Fluorescence and Photocatalytic Properties of a Copper Compound with 2â€Phenylâ€1Hâ€1,3,7,8â€tetraazacyclopenta[l]phenanthrene and Silicotungstic Acid. Zeitschrift Fur Anorganische Und Allgemeine Chemie, 2015, 641, 826-830.	0.6	2
105	Noble-metal-free Co <i> <sub>x</sub> </i> P nanoparticles: modified perovskite oxide ultrathin nanosheet photocatalysts with significantly enhanced photocatalytic hydrogen evolution activity. Nanotechnology, 2020, 31, 325401.	1.3	2
106	Synthesis of AuPd/g-C3N4 nanocomposites and their electrochemical properties. IOP Conference Series: Materials Science and Engineering, 2017, 207, 012005.	0.3	0